







Article

Synthesis of Porous Proton Ion Conducting Solid Polymer Blend Electrolytes Based on PVA: CS Polymers: Structural, Morphological and Electrochemical Properties

Muaffaq M. Nofal ¹, Shujahadeen B. Aziz ^{2,3,*}, Jihad M. Hadi ⁴, Rebar T. Abdulwahid ^{2,5}, Elham M. A. Dannoun ⁶, Ayub Shahab Marif ², Shakhawan Al-Zangana ⁷, Qayyum Zafar ⁸, M. A. Brza ⁹ and M. F. Z. Kadir ¹⁰

¹ Department of Mathematics and General Sciences, Prince Sultan University, P.O. Box 66833, Riyadh 11586, Saudi Arabia; muaffaqnofal@gmail.com

² Hameed Majid Advanced Polymeric Materials Research Laboratory, Department of Physics, College of Science, University of Sulaimani, Kurdistan Regional Government, Qlyasan Street, Sulaimani 46001, Iraq; rebar.abdulwahid@univsul.edu.iq (R.T.A.); ayub.shahab@gmail.com (A.S.M.)

³ Department of Civil Engineering, College of Engineering, Komar University of Science and Technology, Kurdistan Regional Government, Sulaimani 46001, Iraq

⁴ Department of Medical Laboratory of Science, College of Health Sciences, University of Human Development, Kurdistan Regional Government, Sulaimani 46001, Iraq; jihad.chemist@gmail.com

⁵ Department of Physics, College of Education, University of Sulaimani, Old Campus, Kurdistan Regional Government, Sulaimani 46001, Iraq

⁶ Associate Director of General Science Department, Woman Campus, Prince Sultan University, P.O. Box 66833, Riyadh 11586, Saudi Arabia; elhamdannoun1977@gmail.com

⁷ Department of Physics, College of Education, University of Garmian, Kalar 46021, Iraq; shakhawan.al-zangana@garmian.edu.krd

⁸ Department of Physics, School of Science, University of Management and Technology, Lahore 54000, Pakistan; qayyumzafar@gmail.com

⁹ Department of Manufacturing and Materials Engineering, Faculty of Engineering, International Islamic University of Malaysia, Kuala Lumpur 53100, Malaysia; mohamad.brza@gmail.com

¹⁰ Centre for Foundation Studies in Science, University of Malaya, Kuala Lumpur 50603, Malaysia; mfzkadir@um.edu.my

* Correspondence: shujahadeenaziz@gmail.com or shujaadeen78@yahoo.com

Received: 10 October 2020; Accepted: 29 October 2020; Published: 30 October 2020



Abstract: In this study, porous cationic hydrogen (H^+) conducting polymer blend electrolytes with an amorphous structure were prepared using a casting technique. Poly(vinyl alcohol) (PVA), chitosan (CS), and NH_4SCN were used as raw materials. The peak broadening and drop in intensity of the X-ray diffraction (XRD) pattern of the electrolyte systems established the growth of the amorphous phase. The porous structure is associated with the amorphous nature, which was visualized through the field-emission scanning electron microscope (FESEM) images. The enhancement of DC ionic conductivity with increasing salt content was observed up to 40 wt.% of the added salt. The dielectric and electric modulus results were helpful in understanding the ionic conductivity behavior. The transfer number measurement (TNM) technique was used to determine the ion (t_{ion}) and electron (t_{elec}) transference numbers. The high electrochemical stability up to 2.25 V was recorded using the linear sweep voltammetry (LSV) technique.

Keywords: porous polymer electrolyte; XRD and morphology; impedance; electrical properties; TNM; LSV

1. Introduction

Solid polymer electrolytes (SPEs) are a rapidly growing area in the field of polymer physics. As the most significant type of polymer electrolytes (PEs), solid polymer electrolytes (SPEs) have gained the interest of researchers globally [1]. Compared to liquid or gel-based PEs, SPEs are generally more desirable due to their characteristics in terms of processability, ionic conductivity, flexibility, light weight, low cost, safety, and durability [2]. These characteristics make SPEs suitable candidates to be employed in a variety of energy storage devices such as computing laptops, cellular phones, electrochromic display devices, fuel cells, sensors, and smart credit cards [3,4]. Nowadays, the host polymers most commonly used by the researchers in the PEs are poly(vinyl alcohol) (PVA) [1–7], chitosan (CS) [8–12], methylcellulose (MC) [13–15], polyethylene oxide (PEO) [16–18], phosphomolybdic acid (PMA) [19], Nafion membranes [20], and sulfonated hydrocarbon [21].

Critical environmental issues including global warming and environmental pollution are mainly linked to human activities, particularly energy production and usage. In this context, researchers have developed new technologies to employ biodegradable polymer membranes in energy devices like dye-sensitized solar cells, fuel cells, and supercapacitors to reduce fossil fuel consumption and promote alternative energy sources [10]. Electron-donating atoms exist in the structures of polymers with functional groups, for instance, CS and PVA. The presence of lone pair electrons in the oxygen or nitrogen atoms is essential for cation and anion dissociation of the added salt, meaning that the functional groups are important complexation sites for coordination of cations [8,10]. Different approaches including polymer blending and using various salts were investigated to overcome the poor conduction of PE systems. As mentioned in the literature, inorganic salts, particularly alkali metal salts, can significantly improve the conductivity of SPEs and make them reliable for many energy device applications, such as lithium-ion batteries and dual-ion capacitors [22–26]. PVA is a semicrystalline polymer with many hydroxyl functional groups attached to its backbone structure. This polymer is widely used because of its interesting properties like biodegradability, nontoxicity, low cost, biocompatibility, high charge storage capacitance, and high stability [27,28]. On the other hand, chitosan (CS) is a well-known biopolymer in nature obtained from partial deacetylation of chitin. Unlike PVA, CS is a natural semicrystalline polymer with a structure containing two reactive polar groups, amino (NH_2) and hydroxyl (OH), which are suitable for modification [29]. Furthermore, the biomedical applications of CS due to its special characteristics, such as facile processability, biodegradability, antibacterial properties, and cost-effectiveness, highlight the eco-benign properties of this natural polymer [30,31]. CS has several promising pharmaceutical uses and has been studied as a new carrier material in drug delivery systems and for its wound healing, fat binding, antibacterial, and hypocholesterolemic effects [32]. Biopolymer-based membranes, for example, CS, carrageenan, and cellulose, are considered as some good alternative materials to improve the performance of fuel cells, since they are eco-friendly and cheap [33]. CS is one of the most suitable materials that can be used as a substitute for the Nafion membrane since it has shown enhanced performance in low-temperature fuel cell applications [34,35]. In addition, CS exhibited good proton conductivity, attractive alcohol barrier property, and thermal stability after it goes through the crosslinking mechanism [34,35].

Mixing two or more polymer materials (known as the polymer blend approach) has been found to be a suitable technique to reduce the crystallinity degree and increase ionic conductivity at room temperature. Kadir et al. reported the potential use of PVA and CS polymers for applications in electrochemical devices [28,36]. In the polymer blend, electrolytes (usually metal salts) are used as ionic conductivity enhancers. Proton-conducting PEs have negatively charged groups attached to the polymer backbone, and the charge carriers in these systems are found to be H^+ ions, which can be obtained from the dissociation of various ammonium salts [36]. During the dissociation process of ammonium salts, the NH_4^+ ions with other anions are obtained [37]. Three hydrogen atoms in the NH_4^+ ion are tightly bonded, whereas the fourth one is weakly bonded and can hop in the polymer host matrix under the influence of an applied electric field [37]. An extensive survey of the literature illustrates that some ammonium salts, such as ammonium nitrate (NH_4NO_3), ammonium chloride

(NH₄Cl), ammonium bromide (NH₄Br), ammonium iodide (NH₄I), and ammonium thiocyanate (NH₄SCN), have been used as dopants since they are good proton (H⁺) providers [2,13–15,27,28,36]. It is crucial to note that some of the ammonium salts, including NH₄SCN, can have hazardous properties, and potential toxicity should be considered during experimental work.

The intensive survey of the literature revealed that the structural and electrochemical properties of PVA/CS/NH₄SCN electrolytes have not been investigated yet. Therefore, in this work, a proton-conducting PE was prepared using low-lattice-energy NH₄SCN salt [38] as a proton provider. In our previous work, we comprehensively showed that it is crucial to consider the lattice energy of salts in the preparation of polymer electrolytes [39]. In the current study, PVA/CS blended system was doped with various amounts of NH₄SCN salt. The structural, morphological, and electrochemical properties of the blended PEs based on PVA/CS were also been investigated in order to understand the structure–property relationships.

2. Experimental

2.1. Material and Preparation of Blended SPE Films

In this work, the polymer blend was prepared from the chitosan (CS) and poly(vinyl alcohol) (PVA). Ammonium thiocyanate (NH₄SCN) salt (purity 99%) and acetic acid (1%) (CH₃COOH) were used as doping salt and solvent, respectively. All chemicals were used as obtained from Sigma-Aldrich without further purification. The solution casting technique was employed to prepare PVA/CS/NH₄SCN blend SPE films from the raw materials. First, 10 mL of acetic acid was added into 990 mL of distilled water. To prepare the electrolyte samples, 0.5 g of CS was dissolved in 30 mL of 1% acetic acid and left for 3 h under stirring with a magnetic stirrer at room temperature. Simultaneously, 0.5 g of PVA was dissolved completely in 20 mL of distilled water for 1 h under stirring with a magnetic stirrer at 80 °C and then allowed to cool down to room temperature. Later, both PVA and CS solutions were mixed in a beaker with a magnetic stirrer through continuous stirring for 4 h to obtain a homogeneous solution. Various amounts of NH₄SCN dopant salt were added to the CS/PVA solutions, separately in different beakers, while stirring continuously for 6 h until clear solutions were obtained. Five samples with different weight percentages of salts, ranging from 10 to 50 wt.% in 10 wt.% steps, were prepared and coded as PCSH1, PCSH2, PCSH3, PCSH4, and PCSH5, respectively. Finally, the mixtures were transferred into uncovered Petri dishes, allowing the solvent to evaporate gradually at ambient temperature for 3 weeks to obtain completely dry SPE films. The films were dried at room temperature to provide solvent-free films and stored in a desiccator with blue silica gel to remove moisture. The thickness of the samples was measured and found to be in the range of 119 to 123 μm. Table 1 summarizes the weight ratios of samples.

Table 1. Designation and composition of poly(vinyl alcohol) (PVA)/chitosan (CS)/NH₄SCN blend solid polymer electrolyte (SPE) systems.

Sample Designation	(PVA) (g)	(CS) (g)	NH ₄ SCN wt%
PCSH1	0.5	0.5	10
PCSH2	0.5	0.5	20
PCSH3	0.5	0.5	30
PCSH4	0.5	0.5	40
PCSH5	0.5	0.5	50

2.2. XRD and FESEM Study

A Siemens D-5000 X-ray diffractometer (Bruker AXS GmbH, Berlin, Germany) at the wavelength (λ) of 1.5406 Å was employed to record the XRD pattern of PVA/CS/xNH₄SCN with operating current and voltage of 40 mA and 40 kV, respectively. The samples were scanned in the step-scan mode with 2θ angle ranging from 10 to 80° with a step size of 0.1°.

The surface morphology and structural properties of the prepared polymer blend electrolyte films were investigated by field-emission scanning electron microscopy (FESEM) (FEI Quanta 200 FESEM) (FEI Company, Hillsboro, OR, USA).

2.3. Electrical Impedance Spectroscopy EIS

The study of electrical impedance behavior of the fabricated blend films was performed using LCR (HIOKI 3531 Z Hi-tester, Nagano, Japan) impedance analyzer in the frequency range of 50 Hz to 5 MHz, which was interfaced to a computer for data acquisition. For this reason, a couple of stainless-steel (SS) electrodes 2 cm in diameter were used as blocking electrodes. These electrodes are provided with special springs to squeeze and maintain the sandwiched film in an optimal pressure. Then, the films were cut into small circles with a diameter of 1.6 cm and sandwiched between the electrodes for dielectric measurements. The Nyquist plots for complex impedance (Z^*) real part Z' and imaginary part Z'' were obtained; from these, the bulk resistance (R_b) for each sample was determined by the intercept with the real axis. Both real and imaginary parts of complex permittivity (ϵ^*) and complex electric modulus (M^*) were also calculated from the impedance data (i.e., Z' and Z'').

2.4. Transfer Number Measurement (TNM)

The V&A instrument DP3003 was employed for measuring the PCSH4 and PCSH5 blend samples through DC polarization technique versus time at room temperature. TNM for each sample was calculated by tracking a digital DC to V&A instrument DP3003 (V & A Instrument, Shanghai, China), while the cell was polarized with an applied voltage of 0.2 V.

2.5. Linear Sweep Voltammetry LSV

The principal goal of utilizing LSV was to evaluate the electrochemical stability of the most conductive film, assess the working potential range, and determine the breakdown voltage at room temperature. This technique was conducted using a Digi-IVY DY2300 potentiostat (Neware, Shenzhen, China) at the scan rate of 10 mV s⁻¹ in the voltage potential range of 0 to 3 V. The films were kept between the SS electrodes in order to keep the sample at ambient temperature.

3. Result and Discussions

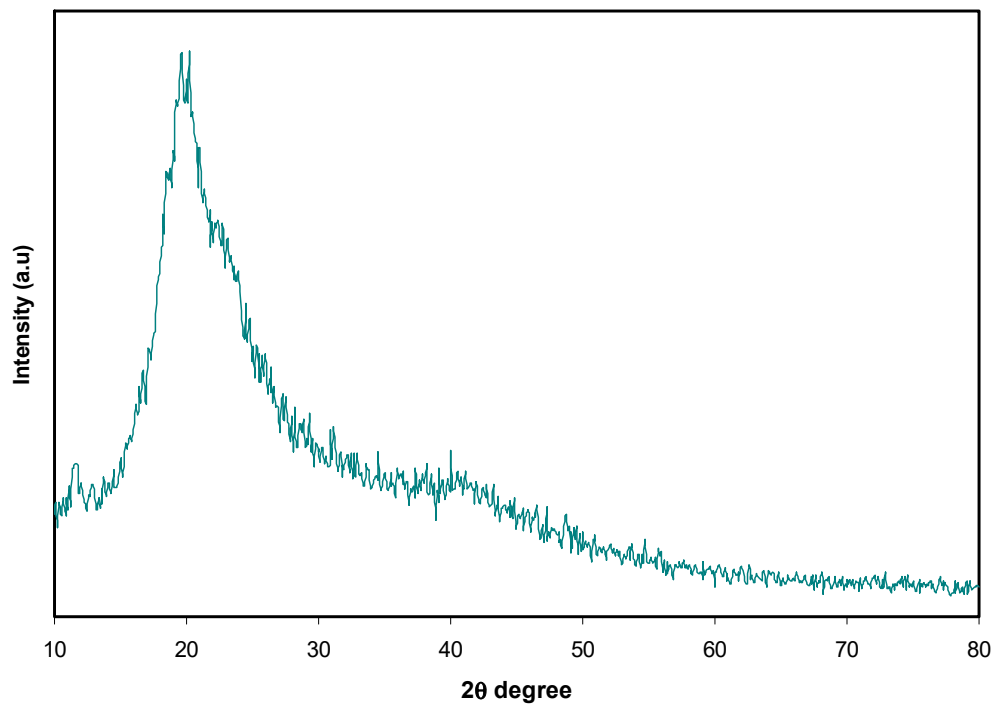
3.1. XRD Analysis

X-ray diffraction is a technique that is widely used to identify amorphous and the crystalline phases of electrolyte film samples. The XRD pattern was used to examine the structural changes of the selected SPE film blends. Figure 1a,b illustrates the X-ray diffraction pattern of pure PVA/CS and doped blend systems at room temperature [15,40]. Both pure PVA and CS exhibit semicrystalline behavior [27]. However, through the blending of these two polymers, the peaks became broader, with a drop in their intensities indicating the increase in the amorphous region in the blended system (as shown in Figure 1a). It can be noticed that the increase of the NH₄SCN salt concentration up to 40 wt.% suppressed the intensity of the peaks of the PVA/CS blend film. This implies that a clear interaction occurred between the dopant salt and the polymer blend, which resulted in the disappearance of the sharp crystalline peaks of the NH₄SCN salt. Further addition of the salt, reaching 50 wt.%, resulted in the appearance of some sharp peaks, which could be related to the occurrence of salt recrystallization. This is related to the salt recrystallization process, which occurred at high NH₄SCN content. For example, a crystalline peak at about $2\theta = 27^\circ$ appeared in PCSH3 and PCSH4 and shifted to $2\theta \approx 28^\circ$ in PCSH5; this peak did not exist in other samples. Similarly, another crystalline peak appeared at around $2\theta = 58^\circ$ for the PCSH5 sample and did not exist in the rest of the samples. These peaks are clear evidence of the recrystallization process at high salt content. These observations are also supported by the results obtained using the FESEM technique showing that the surface roughness of the PCSH5 electrolyte film increased (as discussed in a later section). This is referring to

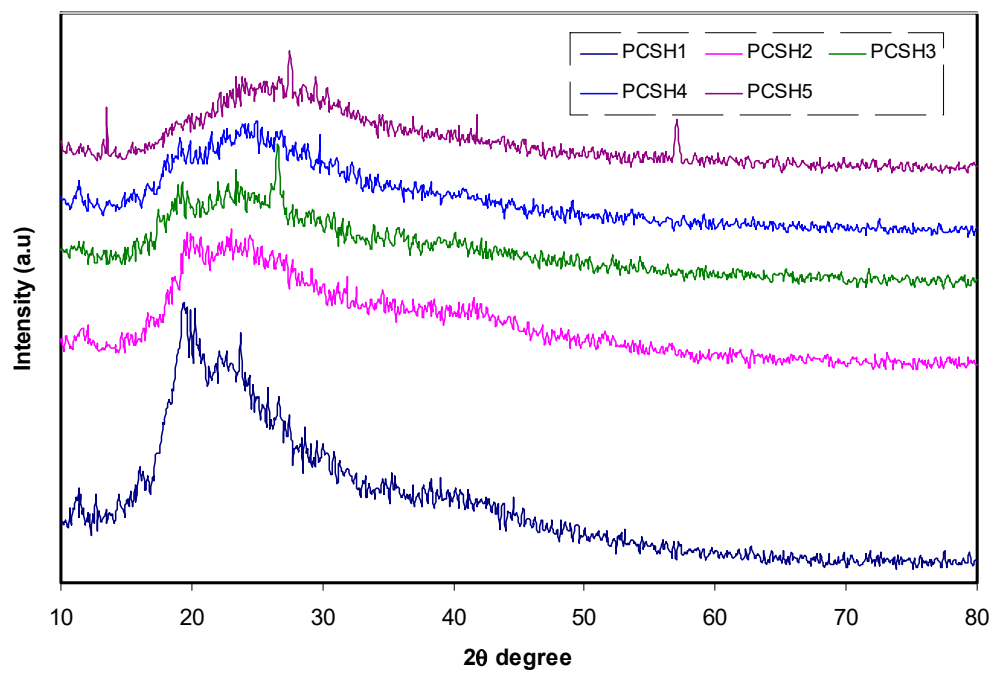
the ion's recombination and formation of ion clusters at the film surface, which caused the loss of a large number of ionic species and the reduction of conductivity [36,41]. Previous studies suggested that the amorphous nature, which is more favorable for the conduction in the PEs, is highlighted by the widening of the X-ray diffraction peaks, also suggesting that the DC ionic conductivity is greater for larger amorphous regions. The variation in the free volume of a polymer influences its molecular motion and physical properties. The polymer blends based on PVA/CS lead to additional free volume, which in turn speeds up the migration of ions at an optimal concentration of the dopant salt. It can be detected that the development of the amorphous region with increasing concentration of the NH_4SCN salt is due to the higher intra- and intermolecular forces of hydrogen bonding, which results in the polymer chain structure having softer nature [42,43]. Thus, the broader peak in the XRD pattern of PCSH4 film electrolyte is considered indicative of some kind of interaction between the blended polar polymer and the dopant salt. The PCSH4 electrolyte had the maximum DC ionic conductivity, as will be discussed later. Finally, the inorganic salt of NH_4SCN has shown a great influence on reducing the crystallinity phases of PVA/CS blended SPEs, since both PVA and CS are semicrystalline polar polymers [8,10].

3.2. Morphology Study

Field-emission scanning electron microscopy (FESEM) is a convenient technique for inspecting the surface composition and morphology of numerous SPE systems [44]. Figure 2a (i–vi) presents the FESEM micrograph images of pure and PVA/CS blends doped with different concentrations of NH_4SCN salt. The FESEM image of pure PVA/CS (Figure 2a (vi)) looks smooth and uniform, which is a good sign of interaction between the blended polymers. It is obvious that the FESEM image of the PCSH1 electrolyte sample shows no porous formation with no phase separation, and the prepared sample appeared to be homogeneous. For the PCSH2 sample, the presence of some white particles on the surface of the film can be observed, which are related to the formation of salt particles without being involved in the ionic conduction process. Moreover, these white particles reduce the ion concentrations that play a vital role in ion-conduction-based electrolytes [41,45]. In fact, as the salt content increased, the surface morphology of the films was changed substantially. Nonetheless, a porous homogenous structure without any protruded particles can be seen for both PCSH3 and PCSH4 samples, which provides more space inside the films with a high surface area. Correspondingly, the more spacious area provides a larger pathway for charge transportation, which is important for ionic conductivity in the PEs [46]. On the other hand, for the highest salt content (50 wt.%), the surface roughness of the electrolyte film increased and its porosity drastically decreased due to the agglomeration of ions, as illustrated schematically in Figure 2b. This can be demonstrated by the fact that the aggregated ions can protrude through the surface of the film. This phenomenon is shown in the XRD pattern where the amorphous region is enlarged as the concentration of the NH_4SCN salt is increased up to 40 wt.% [45,47].



(a)



(b)

Figure 1. X-ray diffraction (XRD) spectra for (a) pure PVA/CS polymer blend and (b) PVA/CS/NH₄SCN electrolyte systems at room temperature.

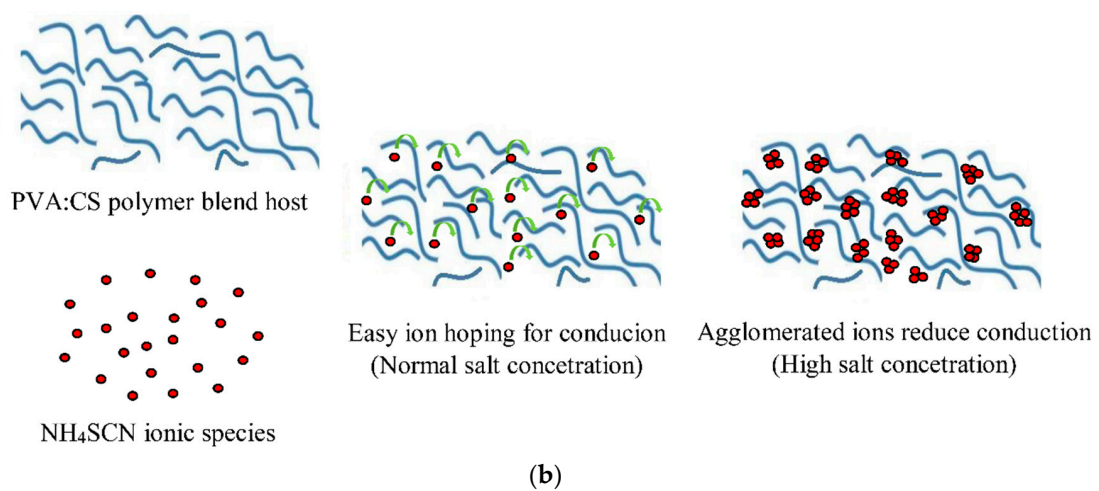
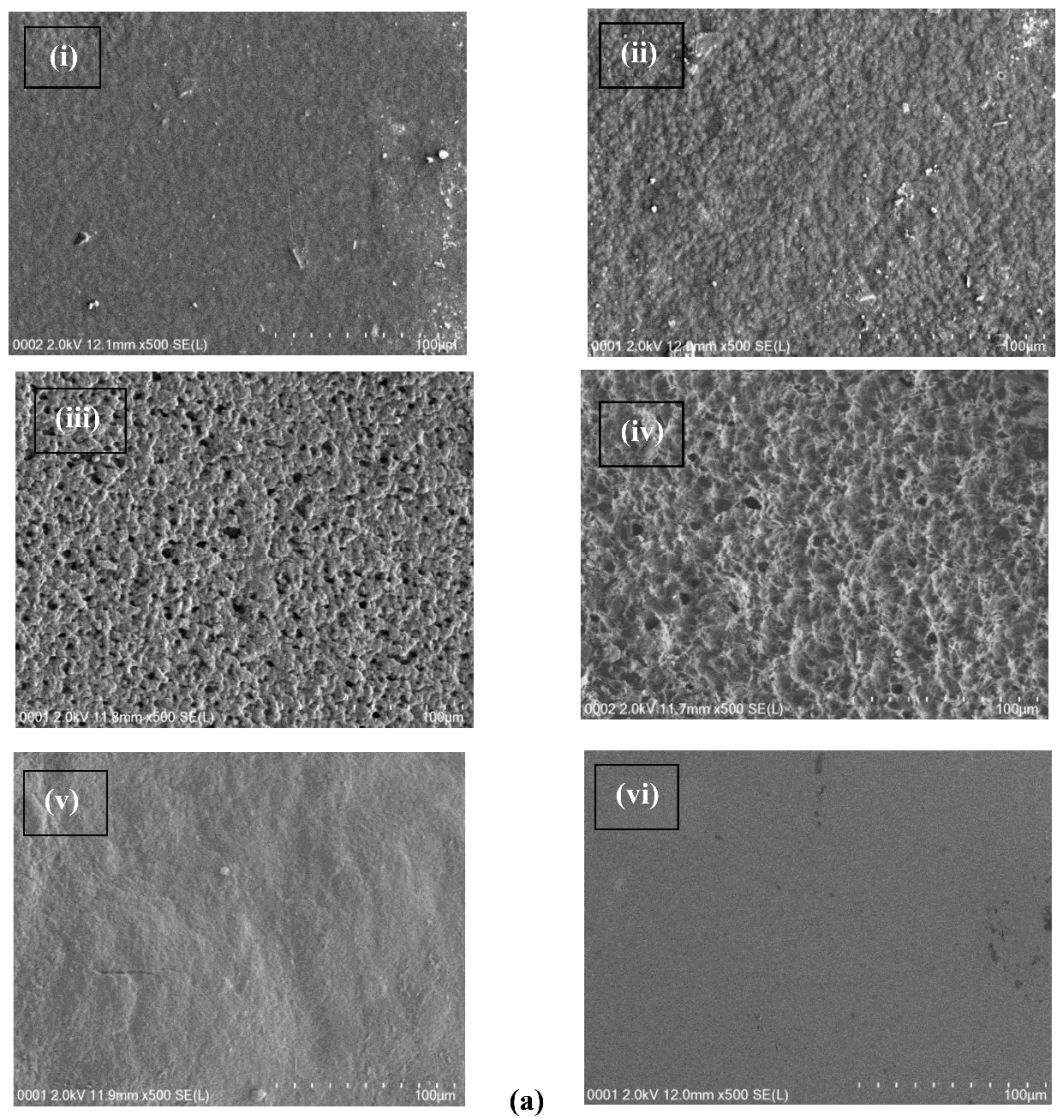


Figure 2. (a) FESEM micrographs of (i) PCSH1, (ii) PCSH2, (iii) PCSH3, (iv) PCSH4, (v) PCSH5, and (vi) pure PVA/CS blend electrolytes. (b) Schematic illustration of ionic transfer in normal NH₄SCN salt concentration and blockage of pathways caused by ion agglomeration in high NH₄SCN salt concentration.

3.3. Impedance Analysis

Electrical impedance spectroscopy (EIS) is considered an effective method for explaining the transference of ions at the sample/electrode interface region and the electrical properties of the electrolyte material. AC impedance analysis can be used to determine the ionic conductivity of the electrolyte films, which mainly depends on the mobility and the density of the charge carriers in the electrolyte films [48,49]. Figure 3a–e illustrates the impedance spectra of the Nyquist plots (Z_i versus Z_r) for all the blended SPE samples at room temperature. Through this technique, the effect of the NH_4SCN dopant salt concentration on the ionic conductivity of the PVA/CS blended samples was explored. It is clear from the Nyquist plots that the half-circle diameter is reduced with the increase of NH_4SCN salt content for the set of the samples up to 40 wt.%. However, upon further addition of NH_4SCN salt up to 50 wt.%, the diameter of the semicircle is increased. This is caused by the agglomeration of ions in the polymer–salt complexes in the system at the highest added salt concentration [14,50,51]. This in turn could reduce the percentage of free space of the charge carriers and lead to a drop in the ionic conductivity of the system. The bulk resistance (R_b) values for all the blended SPE systems were obtained by the intersection of the real axis (Z_r) with the spike line. The value of R_b for the PCSH1 was found to be 4.2×10^5 Ohm, and this value decreased to 10^3 Ohm for the PCSH4 electrolyte sample. Besides, the DC conductivity was calculated using the following relation [52]:

$$\sigma_{dc} = \left[\frac{1}{R_b} \right] \times \left[\frac{1}{A} \right] \quad (1)$$

where t is the thickness of the electrolyte film, A is the area of the electrode, and R_b is the bulk resistance of the material [52]. Moreover, the maximum DC ionic conductivity was found to be $1.48 \times 10^{-5} \text{ S cm}^{-1}$ for the 40 wt.% NH_4SCN doped salt at room temperature (listed in Table 2), which indicates the highest ion mobility with the largest amorphous region among the PCSH electrolyte systems. The impedance spectroscopy outcomes are in good agreement with the FESEM and XRD results. In addition, the ionic conductivity of the system increased as the salt content reached to 40 wt.%. However, at 50 wt.% of NH_4SCN salt, the value of R_b increased and the conductivity decreased due to the recombination of cations and anions of the salt, which dropped the number of movable ions and slowed the motion of ions in the polymer blend network [53]. In polymer electrolytes containing ammonium salts, protons (H^+) are transported by means of the Grotthuss mechanism [54]. As mentioned in Section 1, one of the hydrogen atoms is weakly bonded and can jump in the polymer matrix under the influence of an external electric field [37]. The mobility of the H^+ ion from one site to another is a chance outcome in which the mobile H^+ ion is replaced by another proton from an adjacent site. This is the Grotthuss mechanism where proton transfer happens through proton replacement between the polymer–salt complexed sites [54]. In comparison, the maximum DC ionic conductivity for a CS/PVA/ NH_4NO_3 system was reported to be $2.07 \times 10^{-5} \text{ S cm}^{-1}$ by Kadir et al. [36], which is very close to the DC conductivity value found in this study. In addition, the DC conductivity for a CS/PVA/ NH_4I system was found to be $1.77 \times 10^{-6} \text{ S cm}^{-1}$ by Buraidah and Arof [27]. Shukur et al. investigated a chitosan/ NH_4Br system without blending with another polymer, and the highest obtained conductivity was $4.2 \times 10^{-7} \text{ S cm}^{-1}$ [55]. All these findings confirm that polymer blending is a proper method to boost the ionic conductivity in the polymer-based electrolytes.

Table 2. The DC conductivity value of PVA/CS/ $x\text{NH}_4\text{SCN}$ systems.

Sample Code	DC Conductivity (S/cm)
PCSH1	$(3.43 \times 10^{-8}) \pm 0.32$
PCSH2	$(4.84 \times 10^{-7}) \pm 0.54$
PCSH3	$(2.76 \times 10^{-6}) \pm 0.29$
PCSH4	$(1.36 \times 10^{-5}) \pm 0.19$
PCSH5	$(3.49 \times 10^{-6}) \pm 0.39$

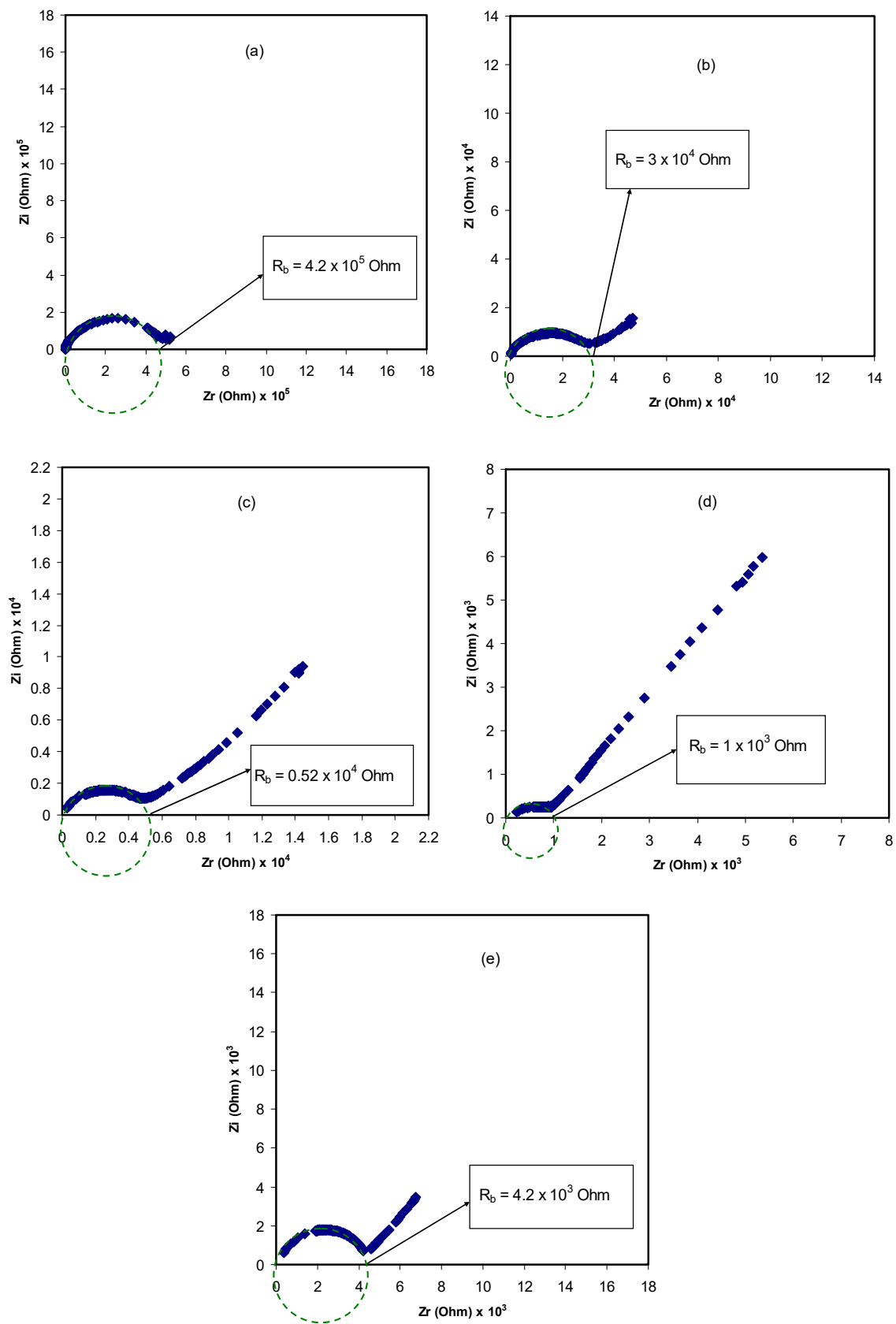


Figure 3. Impedance plot (Z_i versus Z_r) of blended solid polymer electrolytes at room temperature for (a) PCSH1, (b) PCSH2, (c) PCSH3, (d) PCSH4, and (e) PCSH5.

3.4. Dielectric and Electrical Modulus Study

Dielectric properties give information on the ionic transference mechanism in a polymer-based electrolyte. Through these properties, the effect of polarization and nature of the ion conduction inside the electrolyte films can be characterized [46,56]. In addition, the nature of interactions between blended polymers has been evaluated using this technique [46,56]. For the PCSH blended SPE systems, the dielectric properties were determined based on the plots of dielectric parameters (ϵ' , ϵ''). These plots are generated from the impedance data (i.e., Z' and Z'') by utilizing the following equations [56]:

$$\epsilon' = \frac{Z''}{\omega C_0 (Z'^2 + Z''^2)} \quad (2)$$

$$\epsilon'' = \frac{Z'}{\omega C_0 (Z'^2 + Z''^2)} \quad (3)$$

where ω is the angular frequency of the applied field ($\omega = 2\pi f$); ϵ' and ϵ'' are the dielectric constant and dielectric loss, respectively; and C_0 is the vacuum capacitance, which is given by $\epsilon_0 A/t$, where ϵ_0 is the permittivity of free space, A is the electrode cross-sectional area, and t is the film thickness. Figure 4a,b presents the real part (ϵ') and the imaginary part (ϵ'') of the dielectric parameters as a function of frequency at room temperature for the polymer blend electrolyte samples. It can be observed that the dielectric permittivity parameters (ϵ' , ϵ'') are maximum at low-frequency regions owing to electrode polarization (EP) and high density of charge carriers [56–58]. In contrast, at the high-frequency region (>10 kHz), the values of dielectric permittivity are significantly not dependent on frequency. A sharp rise in the dielectric constant (ϵ') was particularly recorded for the PCSH4 electrolyte due to the existence of the high number of ions and maximum ionic conductivity. The PCSH1 exemplified roughly constant behavior, whereas the PCSH2 showed a steady increase. Correspondingly, the ion dispersion was reduced as the dielectric constant dropped quickly at the high-frequency region, decaying to a constant value of 1.2 when $\log(f)$ reached above 4 [59,60]. It is obvious in Figure 4a as the amount of the doped salt increased up to 40 wt.% of NH_4SCN , the value of the dielectric constant gradually increased. However, for 50 wt.%, the values of the dielectric constant (ϵ') dropped due to the aggregation of ions and the decrement of DC conductivity [44,51].

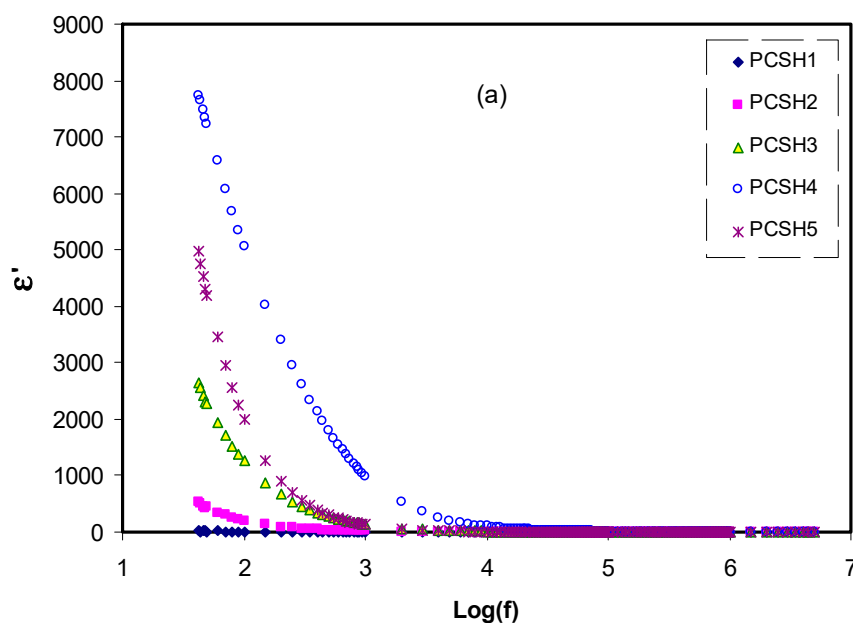


Figure 4. Cont.

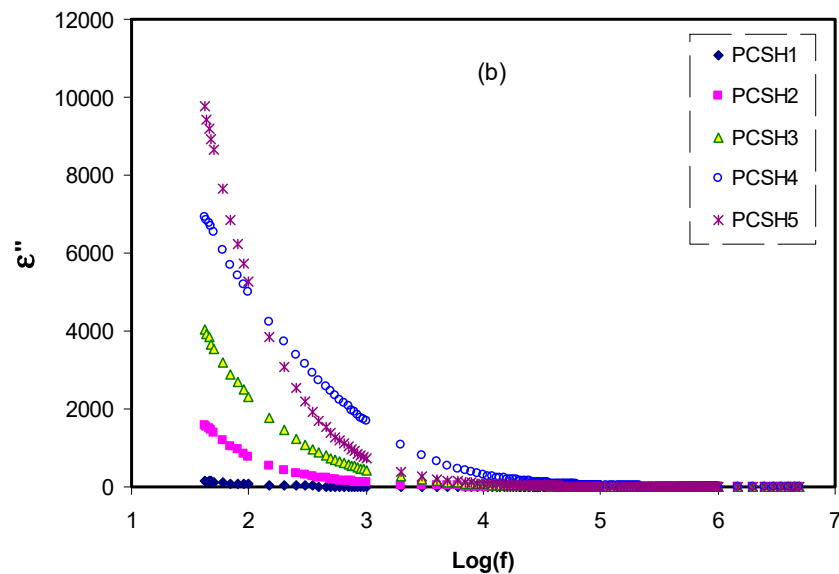


Figure 4. Variation of (a) dielectric constant (ϵ') and (b) dielectric loss (ϵ'') with frequency for the polymer blend electrolyte samples.

In addition, the electric modulus was determined to better understand the conductivity and bulk relaxation process in the blended SPE systems. Through the electrical modulus formalism, space charge phenomena and electrode polarization (EP) problems can be diminished, since it is the reciprocal of the dielectric complex and can be used to minimize the effect of electrode polarization at the high-frequency region. The imaginary (M_i) and real parts (M_r) of complex modulus (M^*) of PVA/CS/ x NH₄SCN blend SPEs were determined from the impedance data (i.e., Z' and Z'') by utilizing the following relations [56]:

$$M' = \frac{\epsilon'}{(\epsilon'^2 + \epsilon''^2)} = \omega C_0 Z'' \quad (4)$$

$$M'' = \frac{\epsilon''}{(\epsilon'^2 + \epsilon''^2)} = \omega C_0 Z' \quad (5)$$

The frequency dependences of the real part (M_r) and imaginary part (M_i) of electric modulus are presented in Figure 5a,b for the PCSH electrolyte films versus frequency at room temperature [61,62]. It is clear that the values of both real and imaginary parts (i.e., M_r and M_i) are increased at the higher frequency region and reach the maximum value, which is attributed to the decrement of the EP and dielectric constant at the high-frequency region. However, the presence of the relaxation peaks in the imaginary part of electric modulus (M_i) reveals that the PCSH blend electrolytes samples are ionic conductors, which means the behavior is non-Debye type. On the other hand, the low value, almost reaching zero, of both real and imaginary parts (i.e., M_r and M_i) can be observed in the low-frequency regions. This is due to the overthrow of the EP influence [63,64]. In the modulus plots, among the NH₄SCN concentrations, the PCSH4 shows the minimum intensity of modulus, indicating the highest DC ionic conductivity.

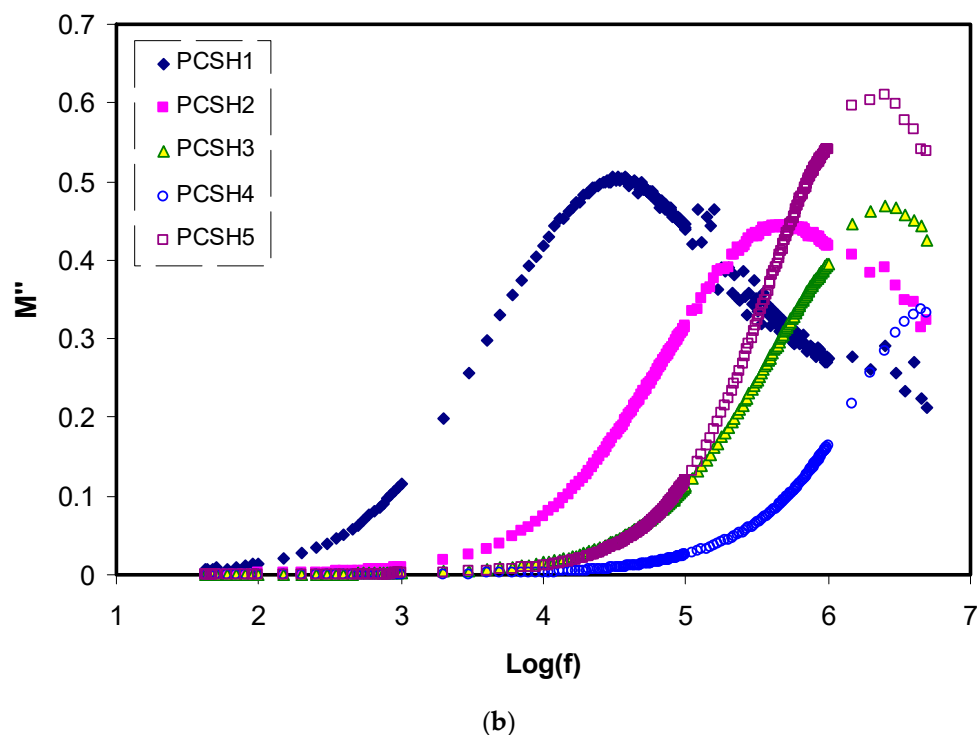
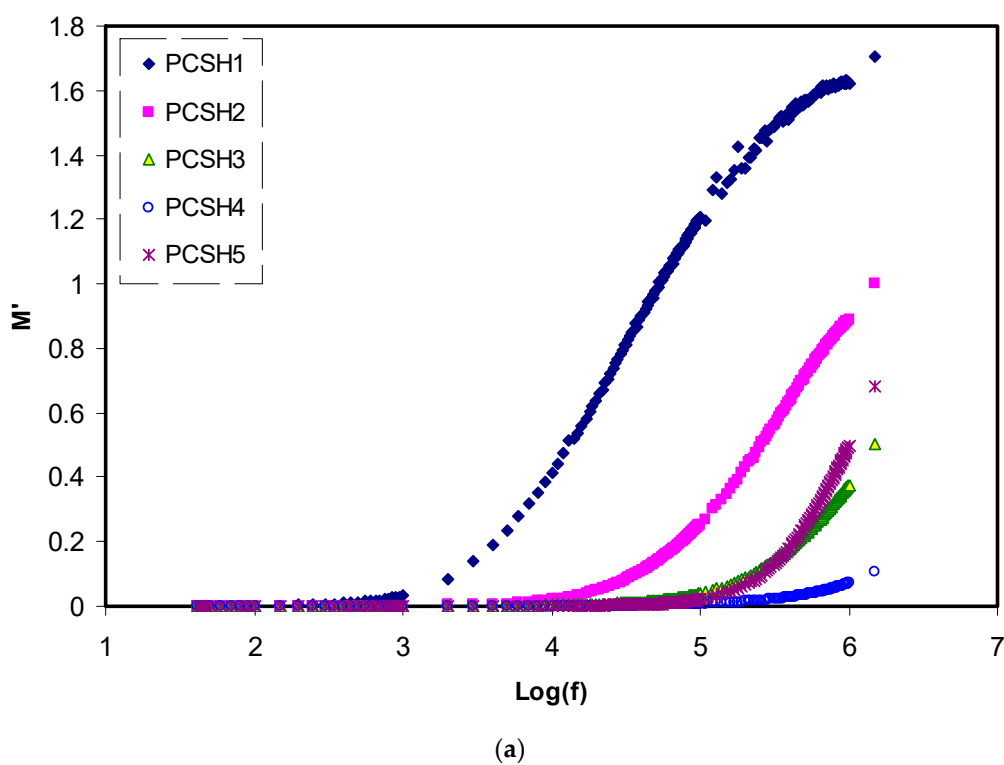


Figure 5. Variation of (a) real part of electric modulus (M_r) and (b) imaginary part of electric modulus (M_i) versus frequency for the polymer blend electrolyte systems at room temperature.

3.5. Transfer Number Measurement (TNM) Study

The TNM technique was employed successfully to estimate the behavior of the particular conduction species in the PVA/CS/ NH_4SCN blend SPE systems using the DC polarization process. Additionally, to confirm the real behavior of the ions in the PCSH blended SPE films, the TNM study

is vital. Regarding this, the nature of ions can be determined by calculating the overall transference number of ions (t_{ion}), which is responsible for the DC ionic conductivity in the polymer-based electrolytes [65,66]. Figures 6 and 7 show the plots of polarization current against time at the applied voltage of 0.2 V for the PCSH4 and the PCSH5 films having 40 wt.% and 50 wt.% NH_4SCN salt added, respectively. Clearly, from the TNM schemes, it can be seen that the initial total current flow dropped quickly and reduced with time. The electrolyte was polarized once it reached the steady state, whereas, the rest of the current stream was a result of electron carriers due to the blocking of cations and anions by stainless-steel (SS) electrodes, which only allow electrons to pass [67–70]. The following equations were used to determine the values of both electron (t_e) and the ion (t_{ion}) transference numbers [38]:

$$t_{ion} = \frac{I_i - I_{ss}}{I_i} \quad (6)$$

$$t_{ion} = 1 - t_e \quad (7)$$

where I_i is the initial current, which is distributed to the ions and electrons, and I_{ss} is the steady-state current that includes electrons only. The result of the ion transference (t_{ion}) was determined from the extracted values of the initial and the steady-state currents for the PCSH4 and PCSH5 conduction samples, which were found to be 0.72 and 0.65, respectively. Therefore, the electron transference (t_e) values were 0.28 and 0.35. Obviously, the results achieved from the TNM study agree with the EIS results in which the most conductive sample (PCSH4) had the maximum DC ionic conductivity [38,71].

The SCN^- anion of the NH_4SCN salt has a large ionic radius of 2.5 Å [72]. Larger-sized ions have lower mobility in comparison with small-size ions as it is difficult for the former to move within the electrolyte and reach the SS electrode surface. This might be the reason for the small value of t_{ion} in the PCSH4 system, which is not very close to the ideal value. Furthermore, the value of the DC conductivity of the most conductive film (PCSH4) is in agreement with the value of the t_{ion} from the TNM analysis.

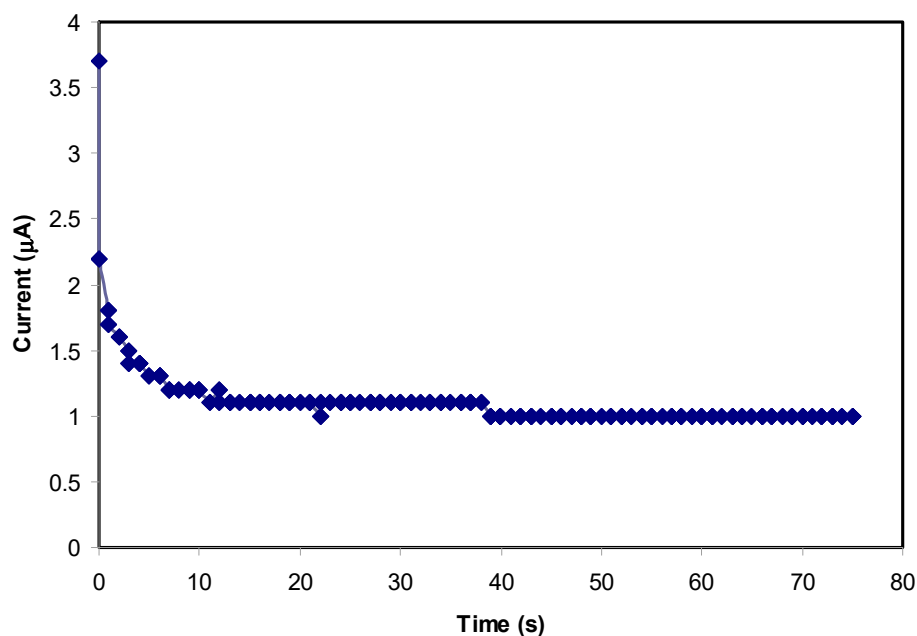


Figure 6. Polarization current for PCSH4 conduction sample versus time.

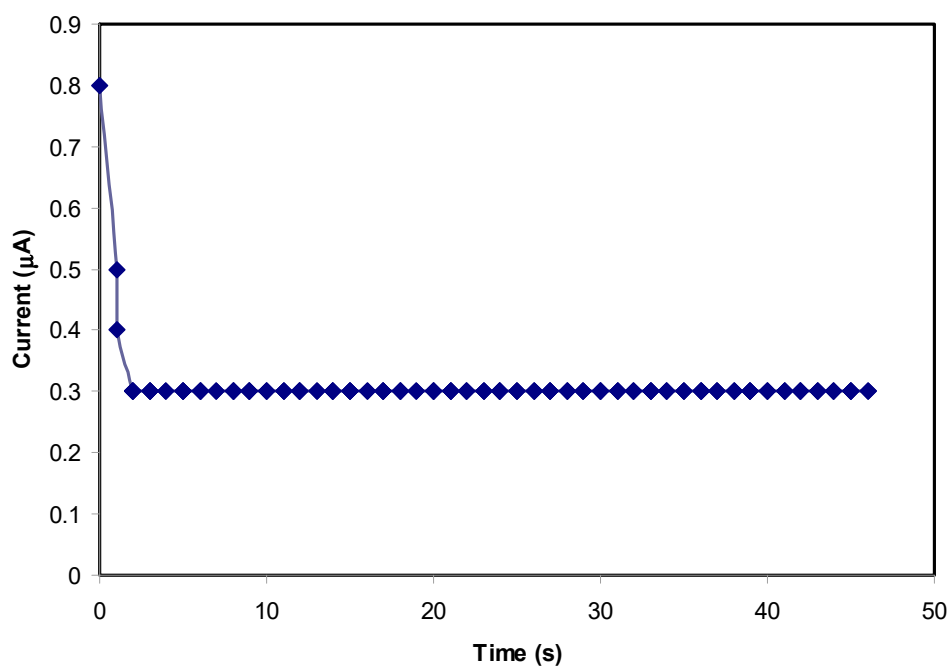


Figure 7. Polarization current for PCSH5 conduction sample versus time.

3.6. Linear Sweep Voltammetry (LSV) Study

Another critical parameter of SPEs used in energy storage device applications is the electrochemical stability. Through employing linear sweep voltammetry (LSV), the electrochemical stability of the largest conducting sample of PVA/CS/NH₄SCN system was investigated at 10 mV s⁻¹. Figure 8 represents the LSV plot of the most conductive PCSH4 film sample at room temperature. A decomposition potential series was measured in the range of 0 to 3 V at the scan rate of 10 mV s⁻¹ for the prepared cells using SS electrodes, in which no clear increase in the value of current was observed up to 2.25 V [73–75]. The decomposition voltage of the sample was calculated to be 2.25 V at ambient temperature. The sharp ascent of the current density was observed beyond 2.25 V, which is due to the decomposition of the sample at the surface of the SS electrodes. A high electrochemical stability window was obtained for the polymers with the presence of a strong electron-withdrawing group [76–78]. The minimum requirement of breakdown voltage for polymer-based electrolytes that can be used in electrochemical device applications is supposed to be ~1 V [17]. Based on the value of the decomposition potential, the PCSH4 film is suitable to be used in energy storage device applications. Table 3 reveals the decomposition voltage for several systems reported in the literature. Previous studies illustrated that in addition to high electrochemical stability, PEs must possess high DC conductivity (10⁻⁵ to 10⁻³ S/cm) to be used for electrochemical device applications [79–81]. In our future work, we will focus on the plasticization of the most conductive system of the present work to improve its DC conductivity and TNM value for energy storage application.

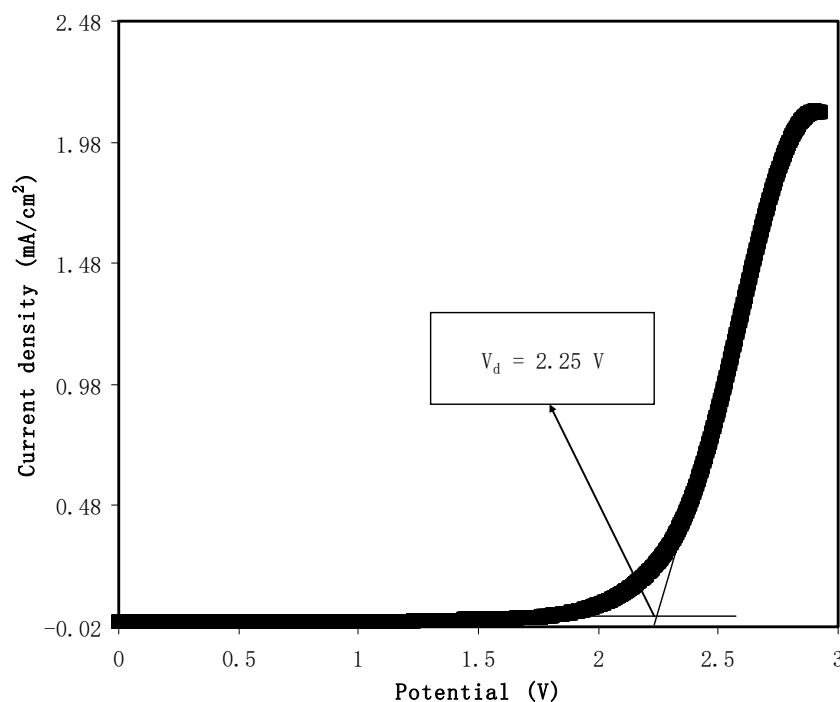


Figure 8. Linear sweep voltammetry plot for the PCSH4 sample at room temperature.

Table 3. The comparison of decomposition voltage of various SPEs.

SPEs	Scan Rate mV s^{-1}	Electrode Material	Decomposition Voltage (V)	References
PVA/dextran/ NH_4I	50	Stainless steel	1.3	[82]
PEO/ $\text{NH}_4\text{SCN}/\text{CeO}_2$	5	Stainless steel	1.4	[83]
PVA/CS/ NH_4Br	1	Stainless steel	1.57	[84]
PVA/CS/ $\text{NH}_4\text{NO}_3/\text{EC}$	10	Stainless steel	1.7	[85]
CS/PS/ NH_4F	100	Stainless steel	1.78	[86]
CS/ $\text{AgNO}_3/\text{Al}_2\text{O}_3/\text{glycerol}$	10	Stainless steel	1.8	[87]
MC/PS/ $\text{NH}_4\text{NO}_3/\text{glycerol}$	1	Stainless steel	1.88	[88]
MC/PS/ LiClO_4	5	Stainless steel	2	[89]
CS/MC/ NH_4I	10	Stainless steel	2.1	[90]
PVA/proline/ NH_4SCN	1	Stainless steel	3.61	[91]
PVA/proline/ NH_4Cl	1	Stainless steel	3.10	[92]
MC/ $\text{NH}_4\text{NO}_3/\text{PEG}$	1	Stainless steel	2.4	[93]
PVA/CS/ NH_4SCN	10	Stainless steel	2.25	This work

4. Conclusions

In conclusion, the effects of polymer blending technique and NH_4SCN dopant salt on the structure, morphology, and ionic conductivity of the PVA/CS blended SPE have been intensively investigated. Both XRD and FESEM outcomes of the PCSH samples have shown that the polymer blending method allows the blended host polymer to develop a greater free volume, which in turn enhances the ionic mobility. Moreover, it has been shown that the inorganic salt of NH_4SCN has a substantial influence on reducing the crystalline phases of PVA/CS polymer blends. The impedance spectroscopy of the samples revealed that 40 wt.% of NH_4SCN is an optimum doping concentration value, resulting in the PCSH4 film having the highest ionic conductivity ($1.48 \times 10^{-5} \text{ S cm}^{-1}$). It was shown that further increment in the salt content caused the conductivity to drop due to the salt recrystallization. Additionally, dielectric properties (ϵ^* , M^*) and TNM and LSV studies confirmed that the amorphous nature, porosity, and conductivity of the systems were enhanced by increasing the amount of NH_4SCN up to 40 wt.%, which is favorable for electrochemical device applications. Subsequently, the PCSH4 system displayed a high electrochemical stability window of up to 2.25 V through the LSV test. The rise in the dielectric parameters (ϵ' , ϵ'') signifies that the increase in the conductivity is mainly due to the

intensification of the number of ion species. The outcomes of the current study are promising and highlight that choosing the appropriate polymer blend with a suitable amount of dopant salt can make the fabricated solid polymer electrolytes suitable for electrochemical device applications.

Author Contributions: Conceptualization, M.M.N., S.B.A., E.M.A.D., S.A.-Z. and M.F.Z.K.; formal analysis, S.B.A.; investigation, A.S.M.; methodology, S.B.A. and A.S.M.; project administration, M.M.N., S.B.A., M.A.B. and M.F.Z.K.; supervision, S.B.A.; validation, J.M.H., R.T.A. and Q.Z.; writing—review & editing, M.M.N., S.B.A., J.M.H., R.T.A., E.M.A.D., S.A.-Z., Q.Z., M.A.B. and M.F.Z.K. All authors have read and agreed to the published version of the manuscript.

Funding: This research received no external funding.

Acknowledgments: The authors gratefully acknowledge the financial support for this study from Ministry of Higher Education and Scientific Research, Kurdish National Research Council (KNRC), KRG/Iraq.

Conflicts of Interest: The authors declare no conflict of interest.

References

1. Aziz, S.B.; Marif, R.B.; Brza, M.A.; Hamsan, M.H.; Kadir, M.F. Employing of Trukhan model to estimate ion transport parameters in PVA based solid polymer electrolyte. *Polymers* **2019**, *11*, 1694. [[CrossRef](#)] [[PubMed](#)]
2. Hema, M.; Selvasekarapandian, S.; Arunkumar, D.; Sakunthala, A.; Nithya, H. FTIR, XRD and ac impedance spectroscopic study on PVA based polymer electrolyte doped with NH₄X (X = Cl, Br, I). *J. Non-Cryst. Solids* **2009**, *355*, 84–90. [[CrossRef](#)]
3. Yang, C.C.; Lin, S.J.; Wu, G.M. Study of ionic transport properties of alkaline poly(vinyl) alcohol-based polymer electrolytes. *Mater. Chem. Phys.* **2005**, *92*, 251–255. [[CrossRef](#)]
4. Saroj, A.L.; Singh, R.K. Thermal, dielectric and conductivity studies on PVA/Ionic liquid [EMIM][EtSO₄] based polymer electrolytes. *J. Phys. Chem. Solids* **2012**, *73*, 162–168. [[CrossRef](#)]
5. Aziz, S.B.; Abdullah, R.M.; Rasheed, M.A.; Ahmed, H.M. Role of ion dissociation on DC conductivity and silver nanoparticle formation in PVA:AgNt based polymer electrolytes: Deep insights to ion transport mechanism. *Polymers* **2017**, *9*, 338. [[CrossRef](#)] [[PubMed](#)]
6. Polu, A.R.; Kumar, R. Preparation and characterization of pva based solid polymer electrolytes for electrochemical cell applications. *Chin. J. Polym. Sci.* **2013**, *31*, 641–648. [[CrossRef](#)]
7. Farah, N.; Ng, H.; Numan, A.; Liew, C.-W.; Latip, N.; Ramesh, K.; Ramesh, S. Solid polymer electrolytes based on poly(vinyl alcohol) incorporated with sodium salt and ionic liquid for electrical double layer capacitor. *Mater. Sci. Eng. B* **2019**, *251*, 114468. [[CrossRef](#)]
8. Aziz, S.B.; Kadir, M.F.Z.; Abidin, Z.H.Z. Structural, morphological and electrochemical impedance study of CS: LiTf based solid polymer electrolyte: Reformulated arrhenius equation for ion transport study. *Int. J. Electrochem. Sci.* **2016**, *11*, 9228–9244. [[CrossRef](#)]
9. Wang, J.; Song, S.; Gao, S.; Muchakayala, R.; Liu, R.; Ma, Q. Mg-ion conducting gel polymer electrolyte membranes containing biodegradable chitosan: Preparation, structural, electrical and electrochemical properties. *Polym. Test.* **2017**, *62*, 278–286. [[CrossRef](#)]
10. Aziz, S.B.; Abdullah, O.G.; Hussein, S.A. Role of Silver Salts Lattice Energy on Conductivity Drops in Chitosan Based Solid Electrolyte: Structural, Morphological and Electrical Characteristics. *J. Electron. Mater.* **2018**, *47*, 3800–3808. [[CrossRef](#)]
11. Osman, Z.; Ibrahim, Z.A.; Arof, A.K. Conductivity enhancement due to ion dissociation in plasticized chitosan based polymer electrolytes. *Carbohydr. Polym.* **2001**, *44*, 167–173. [[CrossRef](#)]
12. Aziz, N.A.; Majid, S.R.; Arof, A.K. Synthesis and characterizations of phthaloyl chitosan-based polymer electrolytes. *J. Non-Cryst. Solids* **2012**, *358*, 1581–1590. [[CrossRef](#)]
13. Aziz, S.B.; Brza, M.A.; Mishra, K.; Hamsan, M.H.; Karim, W.O.; Abdullah, R.M.; Abdulwahid, R.T. Fabrication of high performance energy storage EDLC device from proton conducting methylcellulose: Dextran polymer blend electrolytes. *J. Mater. Res. Technol.* **2019**, *9*, 1–14. [[CrossRef](#)]
14. Samsudin, A.S.; Lai, H.M.; Isa, M.I.N. Biopolymer materials based carboxymethyl cellulose as a proton conducting biopolymer electrolyte for application in rechargeable proton battery. *Electrochim. Acta* **2014**, *129*, 1–13. [[CrossRef](#)]

15. Salleh, N.S.; Aziz, S.B.; Aspanut, Z.; Kadir, M.F.Z. Electrical impedance and conduction mechanism analysis of biopolymer electrolytes based on methyl cellulose doped with ammonium iodide. *Ionics* **2016**, *22*, 2157–2167. [[CrossRef](#)]
16. Kesharwani, P.; Sahu, D.K.; Mahipal, Y.K.; Agrawal, R.C. Conductivity enhancement in K⁺-ion conducting dry Solid Polymer Electrolyte (SPE): [PEO: KNO₃]: A consequence of KI dispersal and nano-ionic effect. *Mater. Chem. Phys.* **2017**, *193*, 524–531. [[CrossRef](#)]
17. Pratap, R.; Singh, B.; Chandra, S. Polymeric rechargeable solid-state proton battery. *J. Power Sources* **2016**, *161*, 702–706. [[CrossRef](#)]
18. Bandara, T.M.W.J.; Karunathilaka, D.G.N.; Ratnasekera, J.L.; Ajith De Silva, L.; Herath, A.C.; Mellander, B.E. Electrical and complex dielectric behaviour of composite polymer electrolyte based on PEO, alumina and tetrapropylammonium iodide. *Ionics* **2017**, *23*, 1711–1719. [[CrossRef](#)]
19. Santamaria, M.; Pecoraro, C.; Di Franco, F.; Di Quarto, F. Phosphomolybdic acid and mixed phosphotungstic/phosphomolybdic acid chitosan membranes as polymer electrolyte for H₂/O₂ fuel cells. *Int. J. Hydrogen Energy* **2017**, *42*, 6211–6219. [[CrossRef](#)]
20. Gagliardi, G.G.; Ibrahim, A.; Borello, D.; El-Kharouf, A. Composite Polymers Development and Application for Polymer Electrolyte Membrane Technologies—A Review. *Molecules* **2020**, *25*, 1712. [[CrossRef](#)]
21. Higashihara, T.; Matsumoto, K.; Ueda, M. Sulfonated aromatic hydrocarbon polymers as proton exchange membranes for fuel cells. *Polymers* **2009**, *50*, 5341–5357. [[CrossRef](#)]
22. Liu, Z.; Wang, J.; Jia, X.; Li, W.; Zhang, Q.; Fan, L.; Ding, H.; Yang, H.; Yu, X.; Li, X.; et al. Graphene Armored with a Crystal Carbon Shell for Ultrahigh-Performance Potassium Ion Batteries and Aluminum Batteries. *ACS Nano* **2019**, *13*, 10631–10642. [[CrossRef](#)]
23. Liu, Z.; Wang, J.; Ding, H.; Chen, S.; Yu, X.; Lu, B. Carbon Nanoscrolls for Aluminum Battery. *ACS Nano* **2018**, *12*, 8456–8466. [[CrossRef](#)]
24. Feng, Y.; Chen, S.; Wang, J.; Lu, B. Carbon foam with microporous structure for high performance symmetric potassium dual-ion capacitor. *J. Energy Chem.* **2020**, *43*, 129–138. [[CrossRef](#)]
25. Liu, Z.; Wang, J.; Lu, B. Plum pudding model inspired KVPO₄F@3DC as high-voltage and hyperstable cathode for potassium ion batteries. *Sci. Bull.* **2020**, *65*, 1242–1251. [[CrossRef](#)]
26. Fan, L.; Ma, R.; Zhang, Q.; Jia, X.; Lu, B. Graphite Anode for a Potassium-Ion Battery with Unprecedented Performance. *Angew. Chem. Int. Ed.* **2019**, *58*, 10500–10505. [[CrossRef](#)]
27. Buraidah, M.; Arof, A. Characterization of chitosan/PVA blended electrolyte doped with NH₄I. *J. Non-Cryst. Solids* **2011**, *357*, 3261–3266. [[CrossRef](#)]
28. Kadir, M.; Aspanut, Z.; Majid, S.; Arof, A.K. FTIR studies of plasticized poly(vinyl alcohol)–chitosan blend doped with NH₄NO₃ polymer electrolyte membrane. *Spectrochim. Acta Part A Mol. Biomol. Spectrosc.* **2011**, *78*, 1068–1074. [[CrossRef](#)]
29. Mobarak, N.; Ahmad, A.; Abdullah, M.; Ramli, N.; Rahman, M.Y.A. Conductivity enhancement via chemical modification of chitosan based green polymer electrolyte. *Electrochim. Acta* **2013**, *92*, 161–167. [[CrossRef](#)]
30. Pandele, A.M.; Ionita, M.; Crica, L.; Dinescu, S.; Costache, M.; Iovu, H. Synthesis, characterization, and in vitro studies of graphene oxide/chitosan–polyvinyl alcohol films. *Carbohydr. Polym.* **2014**, *102*, 813–820. [[CrossRef](#)]
31. Yilmaz, E. Chitosan: A Versatile Biomaterial. *Adv. Exp. Med. Biol.* **2004**, *553*, 59–68. [[CrossRef](#)] [[PubMed](#)]
32. Ramya, R.; Venkatesan, J.; Kim, S.-K.; Sudha, P.N. Biomedical Applications of Chitosan: An Overview. *J. Biomater. Tissue Eng.* **2012**, *2*, 100–111. [[CrossRef](#)]
33. Rosli, N.A.H.; Shyuan, L.K.; Wong, W.Y.; Yunus, R.M.; Khoon, L.T.; Ahmad, A.; Chong, S.T. Review of Chitosan-Based Polymers as Proton Exchange Membranes and Roles of Chitosan-Supported Ionic Liquids. *Int. J. Mol. Sci.* **2020**, *21*, 632. [[CrossRef](#)]
34. Ikram, S.; Ahmed, S.; Ali, S.W.; Agarwal, H. Chitosan-Based Polymer Electrolyte Membranes for Fuel Cell Applications. In *Organic-Inorganic Composite Polymer Electrolyte Membranes*; Springer: Berlin/Heidelberg, Germany, 2017; Volume 377, pp. 381–398.
35. Ramirez-Salgado, J. Study of basic biopolymer as proton membrane for fuel cell systems. *Electrochim. Acta* **2007**, *52*, 3766–3778. [[CrossRef](#)]
36. Kadir, M.F.Z.; Majid, S.R.; Arof, A.K. Plasticized chitosan-PVA blend polymer electrolyte based proton battery. *Electrochim. Acta* **2010**, *55*, 1475–1482. [[CrossRef](#)]

37. Srivastava, N.; Chandra, S. Studies on a new proton conducting polymer system: Poly(ethylene succinate) + NH_4ClO_4 . *Eur. Polym. J.* **2000**, *36*, 421–433. [[CrossRef](#)]
38. Aziz, S.B.; Abdulwahid, R.T.; Hamsan, M.H.; Brza, M.A.; Abdullah, R.M.; Kadir, M.F.; Muzakir, S.K. Structural, Impedance, and EDLC Characteristics of Proton Conducting Chitosan-Based Polymer Blend Electrolytes with High Electrochemical Stability. *Molecules* **2019**, *24*, 3508. [[CrossRef](#)] [[PubMed](#)]
39. Aziz, S.B.; Abdulwahid, R.T.; Hamsan, M.H.; Brza, M.A.; Abdullah, R.M.; Kadir, M.F.; Muzakir, S.K. Structural, Impedance and Electrochemical Characteristics of Electrical Double Layer Capacitor Devices Based on Chitosan. *Polymers* **2020**, *12*, 1411. [[CrossRef](#)]
40. Amran, N.N.A.; Manan, N.S.A.; Kadir, M.F.Z. The effect of LiCF_3SO_3 on the complexation with potato starch-chitosan blend polymer electrolytes. *Ionics* **2016**, *22*, 1647–1658. [[CrossRef](#)]
41. Shukur, M.F.; Kadir, M.F.Z. Hydrogen ion conducting starch-chitosan blend based electrolyte for application in electrochemical devices. *Electrochim. Acta* **2015**, *158*, 152–165. [[CrossRef](#)]
42. Aziz, S.B.; Hassan, A.Q.; Mohammed, S.J.; Karim, W.O.; Kadir, M.F.Z.; Tajuddin, H.A.; Chan, N.N.M.Y. Structural and optical characteristics of pva:C-dot composites: Tuning the absorption of ultra violet (uv) region. *Nanomaterials* **2019**, *9*, 216. [[CrossRef](#)]
43. Mazuki, N.F.; Majeed, A.A.; Nagao, Y.; Samsudin, A.S. Studies on ionics conduction properties of modification CMC-PVA based polymer blend electrolytes via impedance approach. *Polym. Test.* **2020**, *81*, 106234. [[CrossRef](#)]
44. Aziz, S.B.; Abidin, Z.H.Z. Electrical and morphological analysis of chitosan:AgTf solid electrolyte. *Mater. Chem. Phys.* **2014**, *144*, 280–286. [[CrossRef](#)]
45. Aziz, S.B.; Hamsan, M.H.; Karim, W.O.; Kadir, M.F.Z.; Brza, M.A.; Abdullah, O.G. High proton conducting polymer blend electrolytes based on chitosan: Dextran with constant specific capacitance and energy density. *Biomolecules* **2019**, *9*, 267. [[CrossRef](#)]
46. Liu, J.; Khanam, Z.; Muchakayala, R.; Song, S. Fabrication and characterization of Zn-ion-conducting solid polymer electrolyte films based on PVdF-HFP/Zn(Tf)₂ complex system. *J. Mater. Sci. Mater. Electron.* **2020**, *31*, 6160–6173. [[CrossRef](#)]
47. Machappa, T.; Prasad, M.A. AC conductivity and dielectric behavior of polyaniline/sodium metavanadate (PANI/NaVO₃) composites. *Phys. B Condens. Matter* **2009**, *404*, 4168–4172. [[CrossRef](#)]
48. Aziz, S.B.; Hamsan, M.H.; Kadir, M.F.Z.; Karim, W.O.; Abdullah, R.M. Development of polymer blend electrolyte membranes based on chitosan: Dextran with high ion transport properties for EDLC application. *Int. J. Mol. Sci.* **2019**, *20*, 3369. [[CrossRef](#)]
49. Siddaiah, T.; Ojha, P.; Gopal, N.O.; Ramu, C.; Nagabhushana, H. Thermal, structural, optical and electrical properties of PVA/MAA:EA polymer blend filled with different concentrations of Lithium Perchlorate. *J. Sci. Adv. Mater. Devices* **2018**, *3*, 456–463. [[CrossRef](#)]
50. Kumar, D.A.; Selvasekarapandian, S.; Baskaran, R.; Savitha, T.; Nithya, H. Thermal, vibrational and Ac impedance studies on proton conducting polymer electrolytes based on poly(vinyl acetate). *J. Non-Cryst. Solids* **2012**, *358*, 531–536. [[CrossRef](#)]
51. Perumal, P.; Christopher Selvin, P.; Selvasekarapandian, S.; Sivaraj, P. Structural and electrical properties of bio-polymer pectin with LiClO_4 solid electrolytes for lithium ion polymer batteries. *Mater. Today Proc.* **2019**, *8*, 196–202. [[CrossRef](#)]
52. Aziz, S.B.; Karim, W.O.; Ghareeb, H.O. The deficiency of chitosan: AgNO_3 polymer electrolyte incorporated with titanium dioxide filler for device fabrication and membrane separation technology. *J. Mater. Res. Technol.* **2020**, *9*, 4692–4705. [[CrossRef](#)]
53. Premalatha, M.; Vijaya, N.; Selvasekarapandian, S.; Selvalakshmi, S. Characterization of blend polymer PVA-PVP complexed with ammonium thiocyanate. *Ionics* **2016**, *22*, 1299–1310. [[CrossRef](#)]
54. Aziz, S.B.; Karim, O.W.; Qadir, K.W.; Qayyum, Z. Proton ion conducting solid polymer electrolytes based on chitosan incorporated with various amounts of barium titanate (BaTiO_3). *Int. J. Electrochem. Sci.* **2018**, *13*, 6112–6125. [[CrossRef](#)]
55. Shukur, M.F.; Hamsan, M.H.; Kadir, M.F.Z. Investigation of plasticized ionic conductor based on chitosan and ammonium bromide for EDLC application. *Mater. Today Proc.* **2019**, *17*, 490–498. [[CrossRef](#)]

56. Aziz, S.B.; Hamsan, M.H.; Kadir, M.F.Z.; Woo, H.J. Design of Polymer Blends Based on Chitosan:POZ with Improved Dielectric Constant for Application in Polymer Electrolytes and Flexible Electronics. *Adv. Polym. Technol.* **2020**, *2020*, 1–10. [[CrossRef](#)]
57. Ramesh, S.; Ng, H.M.; Shanti, R.; Ramesh, K. Studies on the Influence of Titania Content on the Properties of Poly(vinyl chloride)—Poly (acrylonitrile)-Based Polymer Electrolytes. *Polym. Technol. Eng.* **2013**, *52*, 1474–1481. [[CrossRef](#)]
58. Salman, Y.A. Conductivity and Electrical Properties of Chitosan—Methylcellulose Blend Biopolymer Electrolyte Incorporated with Lithium Tetrafluoroborate. *Int. J. Electrochem. Sci.* **2018**, *13*, 3185–3199. [[CrossRef](#)]
59. Pawlicka, A.; Tavares, F.C.; Dörr, D.S.; Cholant, C.M.; Ely, F.; Santos, M.J.L.; Avellaneda, C.O. Dielectric behavior and FTIR studies of xanthan gum-based solid polymer electrolytes. *Electrochim. Acta* **2019**, *305*, 232–239. [[CrossRef](#)]
60. Aziz, S.B. Study of electrical percolation phenomenon from the dielectric and electric modulus analysis. *Bull. Mater. Sci.* **2015**, *38*, 1597–1602. [[CrossRef](#)]
61. Gozzo, C.; Terezo, A.; Thaines, E.; Sales, A.; Freitas, R.G.; Sombra, A.S.B.; Costa, M. Effects of MgO on dielectric relaxation and phase transition of the ceramic matrix BaBi₄Ti₄O₁₅. *J. Sci. Adv. Mater. Devices* **2019**, *4*, 170–179. [[CrossRef](#)]
62. Aziz, S.B. Occurrence of electrical percolation threshold and observation of phase transition in chitosan(1-x):AgI x (0.05 ≤ x ≤ 0.2)-based ion-conducting solid polymer composites. *Appl. Phys. A* **2016**, *122*. [[CrossRef](#)]
63. Noor, N.A.M.; Isa, M.I.N. Ionic Conductivity and Dielectric Properties of CMC Doped NH₄SCN Solid Biopolymer Electrolytes. *Adv. Mater. Res.* **2015**, *1107*, 230–235. [[CrossRef](#)]
64. Hadi, J.M.; Aziz, S.B.; Mustafa, M.S.; Brza, M.A. Electrochemical Impedance study of Proton Conducting Polymer Electrolytes based on PVC Doped with Thiocyanate and Plasticized with Glycerol. *Int. J. Electrochem. Sci.* **2020**, *15*, 4671–4683. [[CrossRef](#)]
65. Monisha, S.; Mathavan, T.; Selvasekarapandian, S.; Benial, A.M.F.; Aristatil, G.; Mani, N.; Premalatha, M.; Selvasekarapandian, S. Investigation of bio polymer electrolyte based on cellulose acetate-ammonium nitrate for potential use in electrochemical devices. *Carbohydr. Polym.* **2017**, *157*, 38–47. [[CrossRef](#)]
66. Noor, N.A.M.; Isa, M.I.N. Investigation on transport and thermal studies of solid polymer electrolyte based on carboxymethyl cellulose doped ammonium thiocyanate for potential application in electrochemical devices. *Int. J. Hydrogen Energy* **2019**, *44*, 8298–8306. [[CrossRef](#)]
67. Ramlli, M.A.; Isa, M.I.N. Structural and ionic transport properties of protonic conducting solid biopolymer electrolytes based on carboxymethyl cellulose doped with ammonium fluoride. *J. Phys. Chem. B* **2016**, *120*, 11567–11573. [[CrossRef](#)]
68. Manjuladevi, R.; Thamilselvan, M.; Selvasekarapandian, S.; Mangalam, R.; Premalatha, M.; Monisha, S. Mg-ion conducting blend polymer electrolyte based on poly(vinyl alcohol)-poly (acrylonitrile) with magnesium perchlorate. *Solid State Ion.* **2017**, *308*, 90–100. [[CrossRef](#)]
69. Ahmad, N.H.B.; Isa, M.I.N.B.M. Proton conducting solid polymer electrolytes based carboxymethyl cellulose doped ammonium chloride: Ionic conductivity and transport studies. *Int. J. Plast. Technol.* **2015**, *19*, 47–55. [[CrossRef](#)]
70. Sohaimy, M.I.H.; Isa, M.I.N. Ionic conductivity and conduction mechanism studies on cellulose based solid polymer electrolytes doped with ammonium carbonate. *Polym. Bull.* **2017**, *74*, 1371–1386. [[CrossRef](#)]
71. Manjuladevi, R.; Thamilselvan, M.; Selvasekarapandian, S.; Christopher Selvin, P.; Mangalam, R.; Monisha, S. Preparation and characterization of blend polymer electrolyte film based on poly(vinyl alcohol)-poly(acrylonitrile)/MgCl₂ for energy storage devices. *Ionics* **2018**, *24*, 1083–1095. [[CrossRef](#)]
72. Kubota, S.; Ozaki, S.; Onishi, J.; Kano, K.; Shirai, O. Selectivity on Ion Transport across Bilayer Lipid Membranes in the Presence of Gramicidin A. *Anal. Sci.* **2009**, *25*, 189–193. [[CrossRef](#)] [[PubMed](#)]
73. Premalatha, M.; Mathavan, T.; Selvasekarapandian, S.; Selvalakshmi, S.; Monisha, S. Incorporation of NH₄Br in Tamarind Seed Polysaccharide biopolymer and its potential use in electrochemical energy storage devices. *Org. Electron.* **2017**, *50*, 418–425. [[CrossRef](#)]

74. Wang, G.X.; Yang, L.; Wang, J.Z.; Liu, H.K.; Dou, S.X. Enhancement of ionic conductivity of PEO based polymer electrolyte by the addition of nanosize ceramic powders. *J. Nanosci. Nanotechnol.* **2005**, *5*, 1135–1140. [[CrossRef](#)] [[PubMed](#)]
75. Lim, C.S.; Teoh, K.H.; Liew, C.W.; Ramesh, S. Electric double layer capacitor based on activated carbon electrode and biodegradable composite polymer electrolyte. *Ionics* **2014**, *20*, 251–258. [[CrossRef](#)]
76. Aziz, S.B.; Hamsan, M.H.; Brza, M.A.; Kadir, M.F.Z.; Muzakir, S.K.; Abdulwahid, R.T. Effect of glycerol on EDLC characteristics of chitosan: Methylcellulose polymer blend electrolytes. *J. Mater. Res. Technol.* **2020**, *9*, 8355–8366. [[CrossRef](#)]
77. Dhatarwal, P.; Choudhary, S.; Sengwa, R.J. Electrochemical performance of Li⁺-ion conducting solid polymer electrolytes based on PEO–PMMA blend matrix incorporated with various inorganic nanoparticles for the lithium ion batteries. *Compos. Commun.* **2018**, *10*, 11–17. [[CrossRef](#)]
78. Saikia, D.; Wu, H.Y.; Pan, Y.C.; Lin, C.P.; Huang, K.P.; Chen, K.N.; Kao, H.M. Highly conductive and electrochemically stable plasticized blend polymer electrolytes based on PVdF-HFP and triblock copolymer PPG-PEG-PPG diamine for Li-ion batteries. *J. Power Sources* **2011**, *196*, 2826–2834. [[CrossRef](#)]
79. Hamsan, M.; Aziz, S.B.; Kadir, M.; Brza, M.; Karim, W.O. The study of EDLC device fabricated from plasticized magnesium ion conducting chitosan-based polymer electrolyte. *Polym. Test.* **2020**, *90*, 106714. [[CrossRef](#)]
80. Aziz, S.B.; Hamsan, M.H.H.; Nofal, M.M.M.; San, S.; Abdulwahid, R.T.; Saeed, S.R.R.; Brza, M.A.; Kadir, M.F.Z.; Mohammed, S.J.; Al-Zangana, S. From Cellulose, Shrimp and Crab Shells to Energy Storage EDLC Cells: The Study of Structural and Electrochemical Properties of Proton Conducting Chitosan-Based Biopolymer Blend Electrolytes. *Polymers* **2020**, *12*, 1526. [[CrossRef](#)]
81. Azli, A.A.; Manan, N.S.A.; Aziz, S.B.; Kadir, M.F.Z. Structural, impedance and electrochemical double-layer capacitor characteristics of improved number density of charge carrier electrolytes employing potato starch blend polymers. *Ionics* **2020**, *26*, 5773–5804. [[CrossRef](#)]
82. Aziz, S.B.; Brza, M.; Hamsan, M.; Kadir, M.; Muzakir, S.; Abdulwahid, R.T. Effect of ohmic-drop on electrochemical performance of EDLC fabricated from PVA: Dextran: NH₄I based polymer blend electrolytes. *J. Mater. Res. Technol.* **2020**, *9*, 1–12. [[CrossRef](#)]
83. Hadi, J.M.; Aziz, S.B.; Mustafa, M.S.; Hamsan, M.H.; Abdulwahid, R.T.; Kadir, M.F.; Ghareeb, H.O. Role of nano-capacitor on dielectric constant enhancement in PEO:NH₄SCN:xCeO₂ polymer nano-composites: Electrical and electrochemical properties. *J. Mater. Res. Technol.* **2020**, *9*, 9283–9294. [[CrossRef](#)]
84. Yusof, Y.M.; Illias, H.A.; Kadir, M.F.Z. Incorporation of NH₄Br in PVA-chitosan blend-based polymer electrolyte and its effect on the conductivity and other electrical properties. *Ionics* **2014**, *20*, 1235–1245. [[CrossRef](#)]
85. Kadir, M.F.Z.; Arof, A.K. Application of PVA–chitosan blend polymer electrolyte membrane in electrical double layer capacitor. *Mater. Res. Innov.* **2011**, *15*, s217–s220. [[CrossRef](#)]
86. Aziz, S.B.; Hamsan, M.H.; Karim, W.O.; Marif, A.S.; Abdulwahid, R.T.; Kadir, M.F.Z.; Brza, M.A. Study of impedance and solid-state double-layer capacitor behavior of proton (H⁺)-conducting polymer blend electrolyte-based CS:PS polymers. *Ionics* **2020**, *26*, 4635–4649. [[CrossRef](#)]
87. Hadi, J.M.; Aziz, S.B.; Nofal, M.M.; Hussein, S.A.; Hamsan, M.H.; Brza, M.A.; Abdulwahid, R.T.; Kadir, M.F.Z.; Woo, H.J. Electrical, Dielectric Property and Electrochemical Performances of Plasticized Silver Ion-Conducting Chitosan-Based Polymer Nanocomposites. *Membranes* **2020**, *10*, 151. [[CrossRef](#)]
88. Hamsan, M.H.; Aziz, S.B.; Shukur, M.F.; Kadir, M.F.Z. Protonic cell performance employing electrolytes based on plasticized methylcellulose-potato starch-NH₄NO₃. *Ionics* **2019**, *25*, 559–572. [[CrossRef](#)]
89. Yusof, Y.M.; Shukur, M.F.; Hamsan, M.H.; Jumbri, K.; Kadir, M.F.Z. Plasticized solid polymer electrolyte based on natural polymer blend incorporated with lithium perchlorate for electrical double-layer capacitor fabrication. *Ionics* **2019**, *25*, 5473–5484. [[CrossRef](#)]
90. Aziz, S.B.; Hamsan, M.H.; Abdullah, R.M.; Abdulwahid, R.T.; Brza, M.A.; Marif, A.S.; Kadir, M.F.Z. Protonic EDLC cell based on chitosan (CS): Methylcellulose (MC) solid polymer blend electrolytes. *Ionics* **2020**, *26*, 1829–1840. [[CrossRef](#)]
91. Hemalatha, R.; Alagar, M.; Selvasekarapandian, S.; Sundaresan, B.; Moniha, V. Studies of proton conducting polymer electrolyte based on PVA, amino acid proline and NH₄SCN. *J. Sci. Adv. Mater. Devices* **2019**, *4*, 101–110. [[CrossRef](#)]

92. Hemalatha, R.; Alagar, M.; Selvasekarapandian, S.; Sundaresan, B.; Moniha, V.; Boopathi, G.; Selvin, P.C. Preparation and characterization of proton-conducting polymer electrolyte based on PVA, amino acid proline, and NH₄Cl and its applications to electrochemical devices. *Ionics* **2018**, *25*, 141–154. [[CrossRef](#)]
93. Shuhaimi, N.E.A.; Teo, L.P.; Woo, H.J.; Majid, S.R.; Arof, A. Electrical double-layer capacitors with plasticized polymer electrolyte based on methyl cellulose. *Polym. Bull.* **2012**, *69*, 807–826. [[CrossRef](#)]

Publisher’s Note: MDPI stays neutral with regard to jurisdictional claims in published maps and institutional affiliations.



© 2020 by the authors. Licensee MDPI, Basel, Switzerland. This article is an open access article distributed under the terms and conditions of the Creative Commons Attribution (CC BY) license (<http://creativecommons.org/licenses/by/4.0/>).